Target-Driven Moiré Pattern Synthesis by Phase Modulation

Pei-Hen Tsai   Yung-Yu Chuang*
National Taiwan University

Abstract

This paper investigates an approach for generating two grating images so that the moiré pattern of their superposition resembles the target image. Our method is grounded on the fundamental moiré theorem. By focusing on the visually most dominant $(1, -1)$-moiré component, we obtain the phase modulation constraint on the phase shifts between the two grating images. For improving visual appearance of the grating images and hiding capability the embedded image, a smoothness term is added to spread information between the two grating images and an appearance phase function is used to add irregular structures into grating images. The grating images can be printed on transparencies and the hidden image decoding can be performed optically by overlaying them together. The proposed method enables the creation of moiré art and allows visual decoding without computers.

1. Introduction

Moiré patterns are interference patterns created when repetitive structures are overlaid. One property that makes moiré patterns mysterious and interesting is that they consist of new patterns which are clearly visible in the superposition but never appear in any of the original structures [1]. For computer graphics and computer vision, moiré patterns are often unwanted artifacts produced by rendering programs or digital cameras, due to undersampling or unexpected interaction between overlaid structures. Several techniques have been proposed for removing or alleviating their visual impacts. In this paper, we study an opposite problem where moiré phenomenon is not abandoned but utilized for synthesizing the desired patterns. More formally, given a target image, we want to find two grating images so that their superposition resembles the target image through moiré effects but none of each reveals the target image individually.

The moiré phenomenon is intriguing because it is mysterious and unexpected. It seems difficult to control the synthesis of the moiré patterns. Fortunately, for years, scientists have developed techniques for analyzing moiré patterns with the given structures, such as frequency-domain analysis, geometrical approaches and interferometric methods. Our method is grounded on the *fundamental moiré theorem* which, through frequency-domain analysis, provides a mathematical formulation of the moiré components between curvilinear grating images, one kind of repetitive non-periodic grating images (such as L_1 and L_2 in Figure 1). By focusing on the visually most dominating $(1, -1)$-moiré component, we obtain the *phase modulation constraint* which gives the condition of the phase shifts between the two grating images for synthesizing the required target image. Direct application of the phase modulation constraint generates two grating images whose superposition resembles the desired target image. Unfortunately, the grating image alone could also reveal the target image although only obscurely. To make the grating images more uncorrelated to the target image, a smoothness term is used to enforce information spread between the two grating images. Furthermore, an appearance phase function is added for imposing unrelated structures into the grating images and controlling their appearances, making the target image more invisible in each of them.

Our method can be used for several applications such as creating *moiré art*, in which two seemingly unrelated grating images are superposed to reveal an unexpected target image. Figure 1 gives an example[1]. Given "The Starry Night" and "The Scream" as the target images, our method generates two grating images L_1 and L_2. When overlaying L_1 over L_2 with their top edges aligned, the occurred moiré pattern resembles "The Starry Night". When moving L_1 downwards to align its bottom edge with L_2's, "The Scream" shows up. In addition to inciting sense of wonder by moiré art, due to its information hiding nature, our method can also be used for steganography in which the message image is hidden and embedded, and can only be revealed with the key image. Our grating images can be printed on separated transparencies and the decoding can be simply performed by overlaying them together.

[1]The pdf file or printed version could suffer from the sampling problem. The original images of all results can be found in the supplementary.
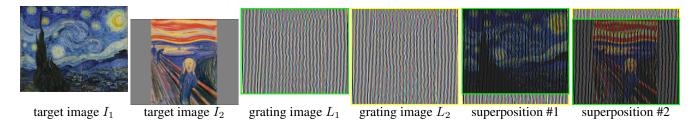
| target image I_1 | target image I_2 | grating image L_1 | grating image L_2 | superposition #1 | superposition #2 |

Figure 1: An example of moiré art created by our method. Given two target images I_1 and I_2, we generate two grating images L_1 and L_2. When overlaying L_1 over L_2 with their top edges aligned, the interference pattern incurred by the moiré phenomenon resembles I_1. By moving L_1 downwards to align its bottom edge with L_2's, the moiré pattern looks like I_2.

2. Related work

Amidror's book "The Theory of the Moiré Phenomenon" provides a comprehensive and thorough treatment of the theory behind moiré phenomenon [1]. It applies Fourier domain approaches to give a detailed analysis for moiré phenomenon caused by periodic patterns and repetitive non-periodic patterns. Our method is built upon the fundamental moiré theorem described in this book.

Lebanon and Bruckstein [6] pioneered in studying synthesis of the desired moiré pattern caused by superposing two generated images. Although both their method and our method build upon the fundamental moiré theorem, with the proposed smoothness term and appearance phase function, the results of our method are visually more promising. Thus, our contributions are the new formulation for optimization and exploration of different schemes for improving visual appearance and hiding capability. Hersch and Chosson [3] proposed a moiré synthesis method for creating dynamic moving moiré patterns when shifting the base band stripe-like layer slowly. Some focused on image hiding in time-averaged moiré [9, 10], the moiré pattern appeared on a fast oscillating image due to persistence of vision.

Huang and Wu [4] proposed a novel visual information concealing technique called "Optical watermarking" where a printed image contains a grid of fine dots and the key contains many vertical stripes. The printed image with the hidden binary image can be decoded by superposing a transparent key image onto it. Our technique shares similarity with optical watermarking. Both use superposition and enhance security by adding irregular structures. However, optical watermarking uses occlusion while our method uses moiré phenomenon. In addition, our method can handle grayscale images while optical watermarking only deals with binary images. Visual cryptography is a technique which allows visual information to be encrypted in such a way that its decryption does not require a computer [11]. Conventional visual cryptography schemes use simple "OR" operation for encryption [7, 2, 5]. They allow the binary share images to be printed on transparencies and decode the binary secret image by overlaying transparencies.

3. Fundamental moiré theorem

This paper takes the spectral approach for analysing the moiré phenomenon [1]. Assume r is the superposition pattern generated by multiplying two layers r_1 and r_2, *i.e.*,

$$r(x, y) = r_1(x, y)\, r_2(x, y). \qquad (1)$$

Using Fourier transform, in the frequency domain, the spectrum of r can be written as:

$$R(u, v) = R_1(u, v) * R_2(u, v), \qquad (2)$$

where the symbol $*$ is the convolution operator and R, R_1 and R_2 are the spectra of r, r_1 and r_2 respectively. Figure 2 gives an example for superposition of two cosine functions with frequency vectors f_1 and f_2. Because of the convolution, the resultant spectrum R contains components whose frequencies do not exist in any of the original spectra R_1 and R_2. The geometric locations of these components in the frequency domain are $f_1 + f_2$, $f_1 - f_2$, $f_2 - f_1$, and $-f_1 - f_2$. Because human vision system is more sensitive to low-frequency contents, a new component becomes noticeable if its frequency is lower than the cutoff and the magnitude is significant enough. These visible components are called moiré patterns.

In this paper, we consider the moiré pattern between repetitive non-periodic grating layers, called *curvilinear gratings*. The curvilinear gratings r_1 and r_2 can be written in the following form:

$$r_1(x, y) = p_1(\phi_1(x, y)), \; r_2(x, y) = p_2(\phi_2(x, y)), \quad (3)$$

where p_1 and p_2 are two one-dimensional periodic profile functions with the period T (we assume $T = 1$ without losing generality); ϕ_1 and ϕ_2 are two phase functions which bend p_1 and p_2 into curvilinear gratings r_1 and r_2. Here, the periodic function p determines the intensity behaviour while the bending function ϕ determines the geometric layout of the grating r. Figure 3 gives examples of gratings in this form. By assigning ϕ_1 and ϕ_2, one can warp the periodic profile p into different gratings r_1 and r_2.

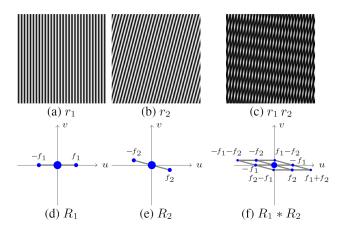(a) r_1 (b) r_2 (c) $r_1\, r_2$

(d) R_1 (e) R_2 (f) $R_1 * R_2$

Figure 2: An example of superposition of two cosine functions $r_1(x,y) = 0.5 + 0.5\cos x$ (a) and $r_2(x,y) = 0.5 + 0.5\cos(x\cos 15° + y\sin 15°)$ (b). In the superposition (c), some low-frequency, nearly horizontal moiré patterns are noticeable. (d) and (e) show the spectra of r_1 and r_2. The dot size indicates the magnitude of a component while the location represents its frequency f and direction θ. The spectrum of the superposition (f) contains additional frequency components due to the convolution. The two components close to the origin ($f_1 - f_2$ and $f_2 - f_1$) correspond to the visible moiré patterns as they are of low-frequency and significant enough.

The fundamental moiré theorem [1] states that the periodic profile and the geometric layout of the moiré are completely independent to each other. Mathematically, it says that the (k_1, k_2)-moiré component m_{k_1,k_2} of the superposition r (here, k_1, k_2 are integers indicating the different moiré components, called *moiré index*) is given by

$$m_{k_1,k_2}(x,y) = p_{k_1,k_2}(\phi_{k_1,k_2}(x,y)). \qquad (4)$$

The bending function ϕ_{k_1,k_2} brings p_{k_1,k_2} into the (k_1, k_2)-moiré appearance and is given by

$$\phi_{k_1,k_2}(x,y) = k_1\phi_1(x,y) + k_2\phi_2(x,y). \qquad (5)$$

The 1-D periodic profile function p_{k_1,k_2} of the (k_1, k_2)-moiré is given by

$$p_{k_1,k_2}(x') = \sum_{n=-\infty}^{\infty} c^{(1)}_{k_1 n} c^{(2)}_{k_2 n} e^{i2\pi n x'}, \qquad (6)$$

where $c^{(1)}_j$ and $c^{(2)}_j$ are Fourier coefficients of p_1 and p_2 at frequency j; since p_1 and p_2 are periodic functions with periods $T = 1$, their Fourier coefficients are non-zero only when j is an integer. In other words, we have $p_{k_1,k_2}(x') = \mathcal{F}^{-1}\{\mathcal{F}\{p_1\}(k_1 u)\mathcal{F}\{p_2\}(k_2 u)\}(x')$. With the fundamental moiré theorem, we can decompose the moiré pattern into several (k_1, k_2)-moiré components whose periodic profiles and bending phase functions can be treated independently.
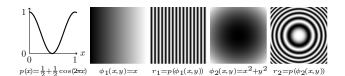

$p(x) = \frac{1}{2} + \frac{1}{2}\cos(2\pi x)$ $\phi_1(x,y) = x$ $r_1 = p(\phi_1(x,y))$ $\phi_2(x,y) = x^2 + y^2$ $r_2 = p(\phi_2(x,y))$

Figure 3: The phase functions ϕ_1 and ϕ_2 bend the profile p into different geometric layouts for the gratings r_1 and r_2.

4. Moiré pattern synthesis

We attempt to solve the following problem: Given a target image I, find two curvilinear grating images L_1 and L_2 such that the moiré pattern of their superposition is close to I. We will impose some desired properties of the gratings for different applications in Section 5, but focus on the basic moiré pattern synthesis problem in this section.

4.1. Moiré pattern of the superposition

We limit our discussions to $(1, -1)$-moiré in this paper because it is visually more dominant than high-order moiré components with $|k_1| > 1$ and $|k_2| > 1$. There are several reasons. First, the high-frequency components of profile functions usually have smaller magnitudes. Therefore, the Fourier coefficients $c^{(1)}_{k_1 n}$ and $c^{(2)}_{k_2 n}$ usually decay very fast with k_1 and k_2. Thus, the periodic profile p_{k_1,k_2} for the (k_1, k_2)-moiré usually has a much smaller range for larger k_1 and k_2, making them less noticeable in the superposition. This indicates that we only need to consider four moiré components, $(1, 1)$, $(-1, -1)$, $(1, -1)$ and $(-1, 1)$. Note that $(1, 1)$ and $(-1, -1)$ moiré are equivalent as they just swap the roles of L_1 and L_2; similar for $(1, -1)$ and $(-1, 1)$ moiré components. Therefore, it leaves us $(1, 1)$ and $(1, -1)$ moiré components which are opposite to each other. Thus, if one is of low frequency, the other will be of high frequency, making it less visually sensible. Therefore, we only manipulate the $(1, -1)$ moiré component and leave other components for free as they are less visually noticeable because of high frequency or low magnitude.

Let $L_1(x,y) = p_1(\phi_1(x,y))$ and $L_2(x,y) = p_2(\phi_2(x,y))$, where the ranges of the profiles are $[0, 1]$ with 2π periods. According to fundamental moiré theorem (Equation 4), the $(1, -1)$-moiré component of their superposition S is:

$$m_{1,-1}(x,y) = p_{1,-1}(\phi_{1,-1}(x,y)), \qquad (7)$$

where the corresponding phase function $\phi_{1,-1}$ and periodic profile $p_{1,-1}$ are given by:

$$\phi_{1,-1}(x,y) = \phi_1(x,y) - \phi_2(x,y), \qquad (8)$$
$$p_{1,-1}(x') = \mathcal{F}^{-1}\{\mathcal{F}\{p_1\}(u)\mathcal{F}\{p_2\}(-u)\}. \qquad (9)$$

For simplicity, we define $m(x,y) \equiv m_{1,-1}(x,y)$, $p_m(x') \equiv p_{1,-1}(x')$ and $\phi_m(x,y) \equiv \phi_{1,-1}(x,y)$ as the moiré component, intensity profile and phase function for the $(1, -1)$-moiré of the superposition S respectively.

(a) I (b) $\hat{I}$

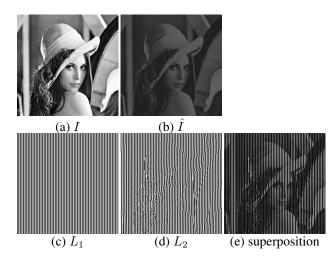(c) L_1 (d) L_2 (e) superposition

Figure 4: A simple example for moiré pattern synthesis. The target image I (a) is first converted into an image $\hat{I}$ (b) with lower contrast by tone mapping. In this example, we used $p_1(x) = p_2(x) = \frac{1}{2} + \frac{1}{2}\cos x$ as periodic profiles. The phase difference Ψ can then be calculated using Equation 12. We fix $\phi_1(x, y) = \frac{1}{2}\pi x$ as the carrier wave L_1 (c). Thus, L_2 can be uniquely determined using Equation 12 and the result is shown in (d). When superposing L_1 and L_2 together, the generated moiré pattern (e) looks similar to the target image $\hat{I}$. Note that, in this example, the target image is slightly visible in L_2. It can be alleviated by distributing the phase difference into L_1 later.

We only discuss grayscale images here. For color images, the same idea is applied to each color channel. Given the target image I and user-specified periodic profiles p_1 and p_2 (their choices will be discussed in Section 4.2), we want that the appearance of $(1, -1)$-moiré m looks similar to I. However, because the range of function p_m is usually smaller than $[0, 1]$, the synthesized moiré cannot match the intensity range of I. Thus, it is necessary to compress the range of I first by some tone mapping operator Γ. Optionally, a low-pass filter f could be applied to prevent messy artifacts in the synthetic images due to high-frequency part in I. Thus, in the following, we use the modified image $\hat{I} = \Gamma(f * I)$ as the target image. The goal is then to synthesize the $(1, -1)$-moiré m such that

$$m(x, y) = p_m(\phi_1(x, y) - \phi_2(x, y)) = \hat{I}(x, y). \quad (10)$$

Thanks to the fundamental moiré theorem, the periodic profile p_m can be pre-determined by the Fourier coefficients of p_1 and p_2 using Equation 9. For $(1, -1)$-moiré component, the periodic profile $p_m(x')$ is a periodic even function for any p_1 and p_2. Thus, the solutions of ϕ_1 and ϕ_2 must satisfy the following equation:

$$\phi_1(x, y) - \phi_2(x, y) = \pm p_m^{-1}(\hat{I}(x, y)) + 2k\pi, k \in \mathbb{Z}, \quad (11)$$

where p_m^{-1} is the inverse function of p_m, which maps an intensity value to the corresponding phase within $[0, 2\pi]$. Note that the $2k\pi$ term in the above equation has no influence on the appearance of L_1 and L_2 because both have the period 2π. In addition, the "$\pm$" sign can be interpreted as exchange of ϕ_1 and ϕ_2. Thus, the constraint on phase difference can be simplified as:

$$\phi_1(x, y) - \phi_2(x, y) = p_m^{-1}(\hat{I}(x, y)) \doteq \Psi(x, y). \quad (12)$$

We call it *phase modulation constraint*. From this constraint, we can interpret $L_1(x, y)$ as a 2D carrier wave and $L_2(x, y)$ as a phase-modulated signal with $\Psi(x, y)$ phase shift. Note that we have the freedom to choose the phase functions ϕ_1 and ϕ_2 as long as their phase shift satisfies the constraint in Equation 12. We will utilize this flexibility for designing better grating images for different applications later. Figure 4 gives an example of the proposed scheme for grayscale images. Note that the target image is slightly visible (although very obscurely) in one of the grating images. We will show how to improve this in Section 5.

4.2. Periodic profile functions

When choosing periodic profiles, we consider the following three factors.

Range of periodic profile of the (1,-1)-moiré component. The most important factor is probably the range of the resulting periodic profile because it directly affects the range of the intensity of the hidden moiré pattern. The periodic profile p_m with a larger range potentially gives a moiré image with better contrast. Figure 5 shows the resulting p_m's for some combinations of different periodic profiles. Among them, p_m from superposing two square wave functions has the largest range. The range of p_m using two cosine functions is not as wide, but good enough in practice.

Magnitude of high-order moiré components. From Equation 6, the periodic profiles p_1 and p_2 not only influence the range of $(1, -1)$-moiré but also magnitude of high-order moiré components. If the periodic profiles p_1 and p_2 contain high-frequency components, they will have more significant high-frequency Fourier coefficients and also significant amplitudes of p_{k_1, k_2} for high-order moiré (where $|k_1| > 1$ and $|k_2| > 1$). Since we ignore high-order moiré in our framework, significant high-order moiré components could inference the target moiré pattern and make it less noticeable. When using square waves as periodic profiles, the amplitude of high-order moiré components are not negligible. Thus, the superposition could contain undesired high-frequency moiré patterns. On the other hand, cosine waves do not have high-frequency components and there is no high-order moiré components when using as profiles.

Appearance of grating images. The periodic profiles also directly affects the appearance of the resultant grating images. Users can design the stripe pattern style of the
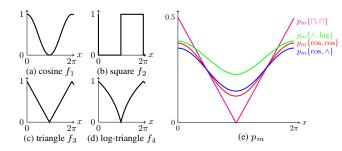
Figure 5: Impacts of periodic functions on the $(1, -1)$-moiré component. (a) a cosine wave $f_1(x) = \frac{1}{2} + \frac{1}{2}\cos x$, (b) a square wave with the period 2π, $f_2(x) = \sqcap_{2\pi}(x)$, (c) a triangle wave with the period 2π, $f_3(x) = \wedge_{2\pi}(x)$, and (d) a triangle wave with the log magnitude, $f_4(x) = \log_4(3 \wedge_{2\pi}(x) + 1)$. In (e), we show p_m's of the superposed periodic profiles from some combinations of these functions. The notation $p_m\{f_a, f_b\}$ in (e) denotes the corresponding p_m for periodic profiles f_a and f_b.

grating images by choosing different profiles. For example, some applications might require binary grating images and the square waves become more suitable.

We used two cosine functions $f(x) = \frac{1}{2} + \frac{1}{2}\cos x$ as the profiles for most cases because they contain less artifacts due to high-order moiré components and have an acceptable range to represent the hidden image with good contrast.

5. Applications and results

The previous section introduces the basic method for synthesizing the moiré pattern so that it looks similar to the target image. Note that we have the luxury to control grating images' appearances by adjusting the phase functions as long as their phase difference satisfies the phase modulation constraint (Equation 12). This section utilizes the luxury to impose desired properties for different applications.

5.1. Moiré art

In the moiré art application, given two target images I_1, I_2 and an offset value Δy, we would like to find two grating images L_1 and L_2 such that (1) the superposition of L_1 and L_2 looks similar to I_1 and (2) after shifting L_1 vertically by Δy pixels, the superposition becomes similar to I_2. Figure 1 gives such an example. Note that, although we only discuss the vertical translation, the same technique could be applied to horizontal shift. By formulating these requirements using Equation 12, we have

$$\begin{cases} \phi_1(x, y) - \phi_2(x, y) = \Psi_1(x, y) \\ \phi_1(x, y) - \phi_2(x, y - \Delta y) = \Psi_2(x, y), \end{cases} \quad (13)$$

where $\Psi_1 = p_m^{-1}(\hat{I}_1)$ and $\Psi_2 = p_m^{-1}(\hat{I}_2)$ are the required phase shifts for appearance resemblance. From this, we

can define the appearance resemblance term E_A using the phase modulation:

$$E_A = \sum_{x,y} \|\phi_1(x, y) - \phi_2(x, y) - \Psi_1(x, y)\|^2$$
$$+ \sum_{x,y} \|\phi_1(x, y) - \phi_2(x, y - \Delta y) - \Psi_2(x, y)\|^2. \quad (14)$$

Note that minimization of E_A does not have a unique solution. If (ϕ_1, ϕ_2) is a solution, then $(\phi_1 + c, \phi_2 + c)$ is also a solution, where c is a constant. To restrict the linear system to have a unique solution, we add an additional constraint $\mathcal{E}$ which requires the first three rows of ϕ_1 and ϕ_2 are as small as possible:

$$\mathcal{E} = \sum_{x, 0 \leqslant y \leqslant 2} \|\phi_1(x, y)\|^2 + \sum_{x, 0 \leqslant y \leqslant 2} \|\phi_2(x, y)\|^2. \quad (15)$$

However, minimizing $E_A + \mathcal{E}$ could lead to vertical discontinuities for every Δy pixels in the grating images as Figure 6(b) shows. Similar discontinuity appears in the superposition as well (Figure 6(c)). It is because we do not enforce the continuity between rows and the constraint of small magnitude cannot propagate from the top to the bottom. Thus, we add a vertical smoothness term E_S:

$$E_S = \left\| \frac{\partial^2 \phi_1}{\partial y^2} \right\|^2 + \left\| \frac{\partial^2 \phi_2}{\partial y^2} \right\|^2. \quad (16)$$

The problem is thus formulated as an energy minimization problem defined as: $E = E_A + \lambda E_S + \mathcal{E}$, where we used $\lambda = 1$ for most cases. Figure 6(d) and (e) show that the smoothness term improves the visual appearance of the grating and superposed images. However, the images could become too blurry if the smoothness term is overemphasized as shown in Figure 6(f) and (g) with λ=10.

One nice property of the system in Equation 13 is that, once we find a set of solution ϕ_1 and ϕ_2, the phase modulation constraint still holds by adding an phase function ϕ_A to both as long as ϕ_A satisfies the following condition:

$$\phi_A(x, y) = \phi_A(x, y + \Delta y) + 2k\pi, k \in \mathbb{Z}. \quad (17)$$

This property allows use to design the appearance of the grating images by adding an appearance phase function ϕ_A. Because the human visual system tends to ignore high-frequency patterns, adding high-frequency appearance phase functions often results in better image hiding quality, as shown in Figure 6(h) and (i). However, when the frequency of ϕ_A is too high, undesired moiré will become noticeable on the grating images due to gridded sampling pattern of image pixels. Adding the appearance phase function could also distort the appearance of the grating images, making the target images even less noticeable. Figure 7 shows an example for controlling the appearance of the grating images and better image hiding with a diagonal stripe pattern as the appearance phase function.
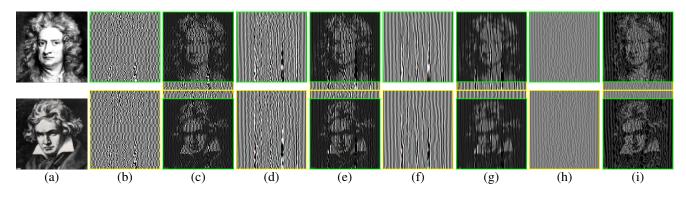
Figure 6: The vertical smoothness term E_S ensures appearance smoothness of the grating and the superposed images. Given the portraits of Newton and Beethoven as targets (a), without E_S (λ=0), both the grating images (b) and the superposed images (c) contain visually disturbing discontinuity. Adding the smoothness term with λ=1 helps reducing the discontinuity as shown in the grating images (d) and superposed images (e). The images could become too blurry if the smoothness is emphasized too much as shown in (f) and (g) with λ=10. An appearance phase function with a higher frequency helps hiding the target images better as seen in the gratings (h) and results (i). However, when the frequency is too high, moiré effects could be observed in the grating images due to insufficient sampling limited by the image resolution.
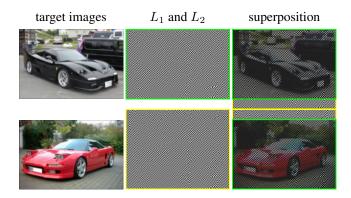
target images L_1 and L_2 superposition

Figure 7: An example of using a diagonal stripe pattern $\phi_A(x,y) = 0.4\pi x + 12\pi y/\Delta y$ as the appearance phase function.

5.2. Moiré cryptography

Cryptography hides information within a carrier. The proposed method can also be used for hiding a secret image within two grating images. The secret image can only be uncovered by their superposition. For this application, it is important to hide the image well so that the secret image cannot be visible with only one of the two grating images. For achieving this goal, in addition to using the smoothness term to spread the information into two gratings, we have also added noise appearance phase functions to make the grating images more difficult to decrypt.

We would like to generate a key image K and a set of information images L_1 to L_N such that, when superposing K on L_i, the moiré pattern looks like the target image I_i. That is, we want $\phi_K(x,y) - \phi_i(x,y) = \Psi_i(x,y)$, where ϕ_K and ϕ_i are the phase functions for the key image and the i-

th information image; and Ψ_i is the required phase shift for synthesizing the i-th target image I_i.

In order to spread information to both K and L_i so that the hidden information is not obvious in either, similar to moiré art, we add a smoothness term and have the following energy function: $\boldsymbol{E} = \boldsymbol{E_A} + \lambda \boldsymbol{E_S} + \mathcal{E}$, where the appearance term $\boldsymbol{E_A}$ is given by:

$$\boldsymbol{E_A} = \sum_{i=1}^{N} \sum_{x,y} \|\phi_K(x,y) - \phi_i(x,y) - \Psi_i(x,y)\|^2; \quad (18)$$

the smoothness term $\boldsymbol{E_S}$ is given by:

$$\boldsymbol{E_S} = \left(\left\|\frac{\partial^2 \phi_K}{\partial x^2}\right\|^2 + \left\|\frac{\partial^2 \phi_K}{\partial y^2}\right\|^2 \right) + \sum_{i=1}^{N} \left(\left\|\frac{\partial^2 \phi_i}{\partial x^2}\right\|^2 + \left\|\frac{\partial^2 \phi_i}{\partial y^2}\right\|^2 \right); \quad (19)$$

and $\mathcal{E}$ restricts the problem to have a unique solution by requiring small values in the upper-left 3×3 corner in ϕ_K and ϕ_i:

$$\mathcal{E} = \sum_{i=1}^{N} \sum_{0 \leqslant x,y \leqslant 2} \|\phi_i(x,y)\|^2 + \sum_{0 \leqslant x,y \leqslant 2} \|\phi_K(x,y)\|^2. \quad (20)$$

A larger λ in the energy function helps hiding the target images better, but resulting in more blur moiré pattern as well.

Even with the smoothness term, the target image could still be slightly visible in the grating images as shown in Figure 8(b) especially when the secret image contains discontinuities. We address this problem by adding an appearance phase function ϕ_A to ϕ_K and ϕ_i's. Unlike moiré art, ϕ_A does not have the requirement in Equation 17 and can be an arbitrary phase function. For better hiding images,

(a) target images
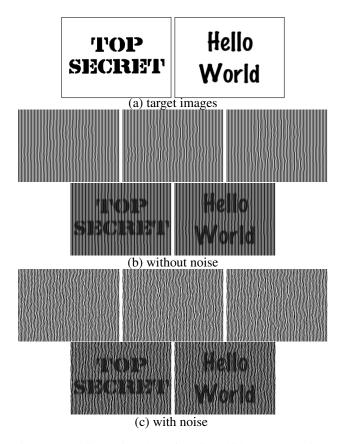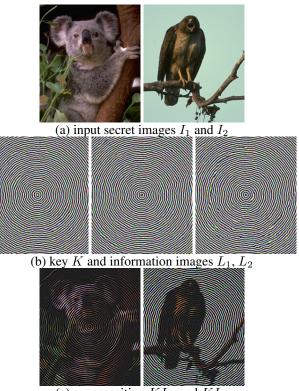
(b) without noise

(c) with noise

Figure 8: Adding noise phase functions hides the target images better. In each sub-figure, the first row shows K, L_1 and L_2 and the second row shows superposed images.

we add a noise function as the appearance phase function. Since the phase functions ϕ_i have been smoothed by the smoothness term, we prefer smooth noise for better visual appearance. We used 2D Perlin noise [8] for this purpose as it is smooth, adjustable and contains visual structures which could better hide the real information. Figure 8 shows the results with the noise appearance function added. Without noise, the embedded images could become visible (Figure 8(b)). With noise, they are better hidden (Figure 8(c)). Figure 9 shows an example in which a wood-grain-like Perlin noise was added as the appearance phase function, making the target even more unrecognizable.

5.3. Optical superposition

One advantage of the proposed approach is that the moiré superposition can be performed without computers. Grating images can be printed on separate transparencies. Superposition can be performed by overlaying the transparencies and the target image will emerge when they are aligned appropriately. We printed L_1 in Figure 6(d) on a transparency and L_2 on a paper. When the transparency was overlaid on the top of the paper at the correct position, the hidden

(a) input secret images I_1 and I_2

(b) key K and information images L_1, L_2

(c) superposition KL_1 and KL_2

Figure 9: Image hiding using a wood-grain-like Perlin appearance function.

image appears. Figure 10 displays the photographs of superposition. Although in principle, grating images need to be perfectly aligned, in practice, we found that the hidden images are still recognizable with imperfect alignments.

Another interesting application would be decrypting with a given pattern. For example, the sampling pattern of the color filter array (CFA) in a digital camera serves as a grating pattern G due to sampling. Given a target image I and a known grating pattern G, we can find the image $L = p_L(\phi_L(x, y))$ by obtaining ϕ_L with

$$\phi_L(x, y) = \phi_G(x, y) + \Psi(x, y), \qquad (21)$$

where ϕ_G is the phase function of G and $\Psi = p_m^{-1}(\hat{I})$. Therefore, given a camera whose CFA sampling pattern G is known, we can obtain L using the above procedure. When displaying L on the screen and capturing it with the camera, we can see the hidden message I in the captured images at proper positions. However, because one of the grating image is given, we do not have the freedom to add appearance phase functions. Thus, the hidden image could be easily recognized from L. Figure 11 shows an example with a RICOH R7 digital camera. The video in the supplementary better demonstrates the result.
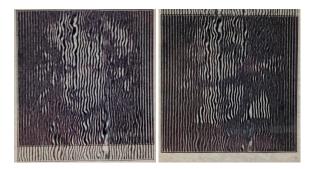
Figure 10: Optical superposition. We printed the two grating images of Figure 6 on a transparency and a paper respectively. When overlaying the transparency on the paper with the top edges aligned, Newton's portrait showed up while Beethoven's emerged when aligning the bottom edges. We show the photographs of superposition here.

(a) grating image   (b) screen captured by the camera

Figure 11: With the known Bayer pattern G of the RICOH R7 digital camera, we can obtain the grating image (a). When displaying it on a LCD screen and capturing with the camera from a proper distance, the hidden image appears in the captured image. Note that the hidden image seems recognizable in the grating image because in this scenario we cannot add a noise phase function.

5.4. Implementation and limitations

The resultant energy functions can be optimized by solving linear systems. For the images shown in the paper, our current unoptimized Matlab implementation (with the standard backslash solver) took roughly two minutes for synthesizing the results.

Because of the limited range of p_m, our method can only generate moiré images with lower contrast. Although tone mapping could enhance the visual quality, the limited range remains a limitation in both theory and practice. Such a limitation could make the hidden images difficult to recognize for some target images. The problem could be made worse when printing out grating images. In addition, we only consider $(1, -1)$-moiré and ignore visual impacts of high-order moiré components. In practice, it is often a valid assumption, especially for the periodic profiles we used. However, in the cases when high-order moiré components become significant, they could disturb the appearance of the

target images and make them less recognizable. Finally, the resolution and frequency content of the hidden images are limited by the process of moiré phenomenon.

6. Conclusions

This paper addresses the problem of designing moiré patterns. We derive the phase modulation constraint and formulate the problem as an energy minimization problem. In addition, we introduce the phase appearance function to further decorrelate the grating images and the target image, making target image invisible in the grating images. Our optimization function is customized for each problem and the phase function can be controlled to decorrelate the target images and grating images. These are the contributions of our paper. While successful in many ways, the effective resolution of the synthesized moiré image is less than the resolution of the target image. In addition, the moiré image has lower contrast and brightness. Nevertheless, even with these limitations, we still find the proposed method useful in many applications.

References

[1] I. Amidror. *The Theory of the Moirè Phenomenon*, volume I: Periodic Layers. Springer, second edition, 2009. 1, 2, 3

[2] G. Ateniese, C. Blundo, A. D. Santis, and D. R. Stinson. Extended capabilities for visual cryptography. *Theoretical Computer Science*, 250(1-2):134–161, 2001. 2

[3] R. D. Hersch and S. Chosson. Band moiré images. *ACM Transactions on Graphics (Proceedings of ACM SIGGRAPH 2004)*, 23(3):239–247, 2004. 2

[4] S. Huang and J. K. Wu. Optical watermarking for printed document authentication. *IEEE Transactions on Information Forensics and Security*, 2(2):164–173, 2007. 2

[5] R. Ito, H. Kuwakado, and H. Tanaka. Image size invariant visual cryptography. *IEICE Transactions on Fundamentals of Electronics, Communications and Computer Sciences*, E82-A(10):2172–2177, 1999. 2

[6] G. Lebanon and A. M. Bruckstein. Variational approach to moirè pattern synthesis. *Journal of the Optical Society of America*, 18(6):1371–1382, 2001. 2

[7] M. Naor and A. Shamir. Visual cryptography. In *Proceedings of EUROCRYPT 1994*, pages 1–12, 1995. 2

[8] K. Perlin. Improving noise. *ACM Transactions on Graphics (Proceedings of ACM SIGGRAPH 2002)*, 21(3):681–682, 2002. 7

[9] M. Ragulskis and A. Aleksa. Image hiding based on time-averaging moirè. *Optics Communications*, 282(14):2752–2759, 2009. 2

[10] E. Sakyte, R. Palivonaite, A. Aleksa, and M. Ragulskis. Image hiding based on near-optimal moirè gratings. *Optics Communications*, 284(1617):3954–3964, 2011. 2

[11] J. Weir and W. Yan. A comprehensive study of visual cryptography. In Y. Shi, editor, *Transactions on Data Hiding and Multimedia Security V*, pages 70–105. Springer-Verlag, 2010. 2